DOI: 10.21062/mft.2024.023 http://www.journalmt.com

Research and Dynamic Analysis of a Cable Reel Device Based on Constant Tension

Hengcan Li (0000-0002-1560-5323)
Mechanics Institute, North China University of Water Resources and Electric Power, Zhengzhou, 450045, China,
E-mail: lic2020522411@yeah.net

A constant tension cable reel based on planetary gear transmission is introduced. The parameters of the mechanism are determined to analyze the speed and torque of the transfer mechanism. The relationship between the thread pitch and cable type show that different cable models require different parameters for the constant tension cable reel. The mechanism is designed to automatically adjust the force required for cable pulling and maintain a constant maximum tension. Then the relationship between the moment and speed of each output shaft is analyzed, and the operation mode of the cable reel was explained. The experimental results show that the proposed cable reel can pull the cable flexibly while providing the required constant tension, without damaging the cable and extending its service life. The pitch of the screw-thread pair is directly related to the required tension of the cable and the cable diameter. If the power supply cable model is different, the parameters of constant tension cable reel are also different.

Keywords: Cable reel, planetary gear, friction disk, constant tension, flexible cable pulling

1 Introduction

The cable reel is widely used in various lifting devices to provide power supply, control power, or control signals. To reliably wrap the cable around the reel, most cable reels nowadays deploy sliding device in the reel drive mechanism, allowing the cable to operate in a large and constant tension. However, this device intensifies the cable wear and shortens its service life [1-2].

To overcome the above problems, a constant tension cable reel is introduced for flexible cable pulling. The cable reel relies on the automatic gear shifting of the transmission mechanism to flexibly pull the cable, maintaining the cable being pulled under a constant maximum tension. The reel provides the required small pulling force to the cable [3-4]. Our cable reel can significantly extend the service life of the cable than the other constant moment cable reels. This device cannot only pull and retract cables flexibly, but also maintain a constant tension of cables during operation. This technology has been recognized as a national invention patent.

2 Operation Principle and Structure Design

Fig. 1 shows the structure of the proposed flexible cable-pulling constant tension cable reel. Lubricating oil is added into housing, ensuring that each rotating component in the housing is always lubricated.

The 2K-H (WW) positive differential planetary transmission consists of the input shaft I, sun wheels a and b, planet wheels d and g, planet carrier H, and output shaft II [5].

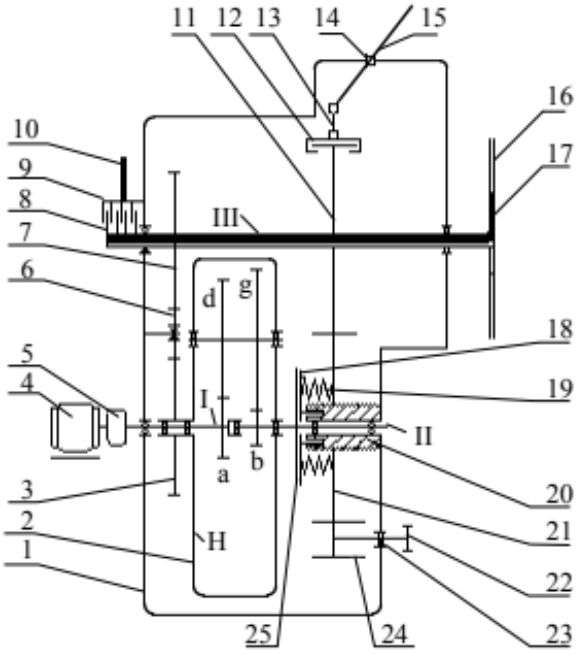

Fig. 1 *Structure of the cable reel*

Where:
1…Housing,
2…2K-H (WW) positive differential planetary transmission [5],
3…GearI,
4…Motor,
5…Worm gear reducer,
6…Transition gear,
7…Gear II,

8…Rotary vane of collector,
9…Static vane of collector,
10…Power line of mobile device,
11…Gear III,
12…Driver plate,
13…Connecting rod,
14…Shaft,
15…Lever,
16…Reel ,
17…Power supply cable,
18…Static friction disk,
19…Pressure spring,
20…Adjustable seat,
21…Adjustable big gear,
22…Adjustable hand wheel,
23…Bearing,
24…Adjustable small gear,
25…Rotary friction disk.

The speed and moment generated by the motor are transmitted to the input shaft I via the worm gear reducer. The speed and moment of the input shaft I is distributed by differential planetary transmission to the output shaft II and the planet carrier H. The speed and moment of the planet carrier H are transmitted to the output shaft III via the gear I, transition gear, and gear II [4].

On the output shaft III, the reel is fixed on the right end, the rotary vane of the collector is fixed on the left end, and the gear III is installed in the middle. The gear III can rotate along with the output shaft III, or slide to the left or right on this shaft. The reel is the pulling and storage device of power supply cable, which adopts the single-row multi-layer storage method [5]. The rotation of output shaft III drives the rotation of the reel and rotary vane of the collector.

After passing through the reel, the power supply cable is connected to the rotary vane of the collector via the hole at the center of the shaft III. The power line of the mobile device 10 is connected to the static vane of the collector. In this way, the fixed power supply can power the mobile device.

The rotary friction disk rotates with the output shaft II. The end pin of static friction disk is inserted into the end hole of the adjustable seat, preventing the friction disk from rotating. Both the outer surface of adjustable seat and the inner hole of the adjustable big gear are threaded. The two components are linked up via threaded connection.

The pressure spring is mounted between the static friction disk and the adjustable big gear. The rotation of the output shaft III drives the rotation of the gear III, which in turn drives the rotation of the adjustable big gear. During the rotation, the adjustable big gear also moves laterally, and relaxes or presses the pressure spring. The friction between the friction pair of the static friction disk and the rotary friction disk is thereby changed, varying the moment of resistance for the output shaft II. The rotation of the adjustable big gear causes the idling of the adjustable small gear and the adjustable hand wheel.

3 Dynamic analysis

The number of teeth $\mathrm{Z_3}$ of gear I is equal to that $\mathrm{Z_7}$ of gear II. Then, the speed of the planet carrier H equals to that of $n_{\mathrm{III}}$of the output shaft III [6]:

$$n_{\mathrm{H}} = n_{\mathrm{III}} \tag{1}$$

The number of teeth $\mathrm{Z_a}$, $\mathrm{Z_b}$, $\mathrm{Z_d}$, and $\mathrm{Z_g}$ are selected for gears a, b, d, and g in 2K-H (WW) positive differential planetary transmission, so that the characteristic parameters of the transmission mechanism satisfy [6]: $\alpha = \frac{\mathrm{Z_d Z_b}}{\mathrm{Z_a Z_g}} = 0.5$.

Then, the speed and moment of the input shaft I and the output shaft II, as well as the planet carrier H respectively satisfy [7-8]:

$$n_I - 0.5n_{\mathrm{II}} - 0.5n_{\mathrm{H}} = 0 \tag{2}$$

$$M_I = -2\,M_{\mathrm{II}} = -2\,M_{\mathrm{H}} \tag{3}$$

Substituting formula (1) into formula (2):

$$n_{\mathrm{I}} - 0.5n_{\mathrm{II}} - 0.5n_{\mathrm{III}} = 0 \tag{4}$$

Formula (2) shows that, when the input shaft I cannot rotate, i.e.,$n_I = 0$, the planet carrier H and output shaft II rotate at the same speed in the opposite directions. Hence, the transmission ratio $n_{\mathrm{H-II}}$ from the planet carrier H to the output shaft II equals 1. Formula (3) shows that, when the motor rotates, the output moment is magnified by the worm gear reducer, and then imported to the input shaft I. The input shaft I evenly allocates the moment to the output shaft II and the planet carrier H. Consequently, the active moment of the output shaft II is always equal to that of the planet carrier H: $M_{\mathrm{II}} = M_{\mathrm{H}}$.

For the static friction disk and the rotary friction disk, the inner and outer radii of the overlapping area are denoted as R_1 and R_2 respectively. The friction coefficient is denoted as μ_1, the number of friction surfaces as Z, the elastic coefficient and compressed distance of the spring as k_1 and L, respectively. Then, the movement of the resistance M'_{II} from the friction disk to the output shaft II can be expressed as [9-10]:

$$M'_{\mathrm{II}} = \mu_1 \mathrm{Z} k_1 L R_V \tag{5}$$

Where, R_V is the equivalent friction radius (mm):

$$R_V = \frac{2(R_2^3 - R_1^3)}{3(R_2^2 - R_1^2)} \tag{6}$$

For the adjustable seat, the nominal diameter of threads on the outer surface is denoted as d_1 (mm), and the tightening moment coefficient as k_2 .

Then, the moment T rotating the adjustable big gear can be expressed as:

$$T = k_2 k_1 L d_1 \tag{7}$$

Then, the ratio m of the movement of resistance M'_{II} of output shaft II to the moment T needed to rotate the adjustable big gear 21 can be expressed as [7]:

$$m = \frac{M'_{\mathrm{II}}}{T} = \frac{\mu_1 \mathrm{Z} R_{\mathrm{V}}}{k_2 d_1} \tag{8}$$

The friction disk is made of the quenched steel, and its $\mu_1$isin the range of 0.05-0.1. The screw-thread pair of the adjustable seat and the adjustable big gear is lubricated fine-finished surfaces. Hence, the value of k_2 could be 0.1. Then, the number of friction surfaces Z and the values of R_1, R_2, and d_1 are selected, and substituted into formula (8). M'_{II} is a multiple of T. Through calculation, it is reasonable to control m between 20 and 40.

During cable pulling, the minimum tension of the power supply cable is the gravity of the cable in its free hanging length (Fig. 2). Since the cable must be wrapped tightly on the reel, it is necessary to apply an initial tension on the cable. The minimum tension N of the cable is the sum of the said gravity and the initial tension. In other words, the dangling length of the pulled cable must be longer than the free hanging length. Fig. 3 shows the wound state of the pulled cable [11-13].

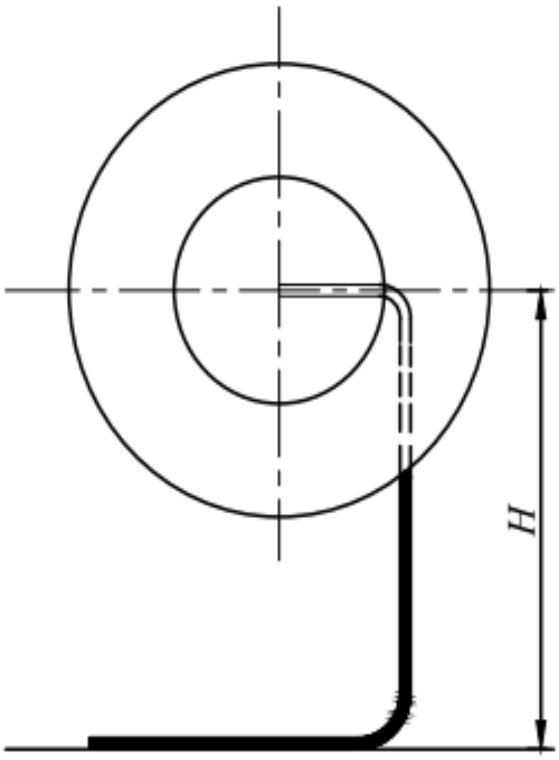

Fig. 2 *Wound state of the cable under minimum tension*

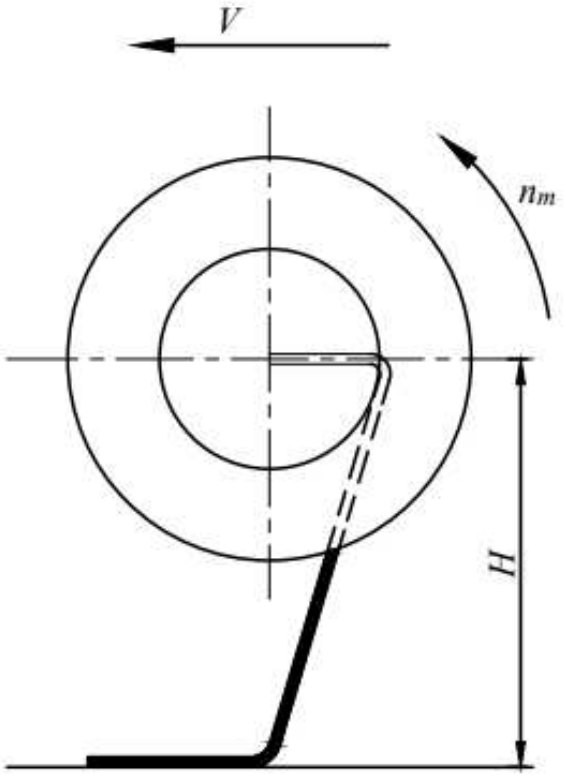

Fig. 3 *Wound state of the cable after being pulled*

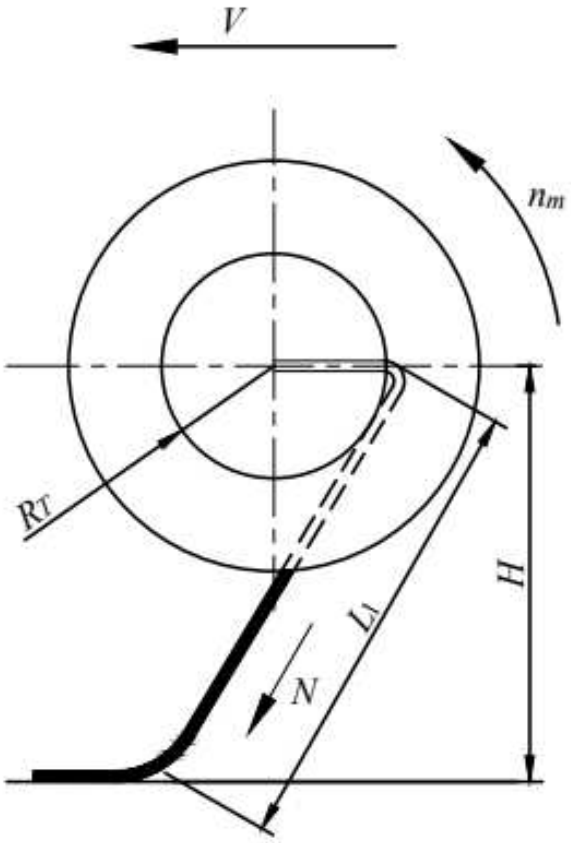

Fig. 4 *Force diagram in the initial state*

When the mobile device is at the start position of the journey, the cable reel is in its initial state (Fig. 4).

In this case, the dangling length L_1 of the cable is adjusted to adjust the tension of the cable to N. Then, the moment of resistance $M_O^{'}$ of the reel can be expressed as:

$$M_O^{'} = NR_0 = N\left(R_T + \frac{d_2}{2}\right) \quad (9)$$

Where:

R_T…The radius of the outer circle of the contact between the reel and the cable,

d_2…The diameter of power supply cable.

Suppose the compressed distance of spring 19 is L_0 at the start position in Fig. 4. By formula (7), the moment T_0 rotating the adjustable big gear can be expressed as [12-13]: $T_0 = k_2k_1L_0d_1$.

It is assumed that the number of teeth Z_{11} of the gear III is equal to that of the adjustable big gear. Then, the transmission ratio n_{11-21} from the gear III to the adjustable big gear is $n_{11-21} = \frac{Z_{21}}{Z_{11}} = 1$. Therefore the moment of resistance $M_{11,0}^{'}$ of the gear III can be expressed as:

$$M_{11,0}^{'} = \frac{T_0}{n_{11-21}} = k_2k_1L_0d_1 \quad (10)$$

Without considering any frictional loss, the moment of resistance $M_{\mathrm{III},0}^{'}$ of the output shaft III can be expressed as:

$$M_{\mathrm{III},0}^{'} = M_O^{'} + M_{11,0}^{'} = N\left(R_T + \frac{d_2}{2}\right) + k_2k_1L_0d_1 \quad (11)$$

Since gears I and II have the same number of teeth, and the frictional loss is neglected, the moment of resistance of the output shaft III will be entirely transmitted to the planet carrier H. Therefore, the moment of resistance $M_{\mathrm{H},0}^{'}$ of the planet carrier H can be expressed as [14-15]:

$$M_{\mathrm{H},0}^{'} = M_{\mathrm{III},0}^{'} = N\left(R_T + \frac{d_2}{2}\right) + k_2k_1L_0d_1 \quad (12)$$

According to formula (8), the moment of resistance of the output shaft II can be expressed as:

$$M_{\mathrm{II},0}^{'} = mT_0 = mk_2k_1L_0d_1 \quad (13)$$

Let formula (12) equal to formula (13):

$$L_0 = \frac{N\left(R_T + \frac{d_2}{2}\right)}{(m-1)k_2k_1d_1} \quad (14)$$

Since m belongs to [20, 40], when (m -1) is replaced with m, i.e., the moment of resistance of the adjustable big gear to the output shaft III is overlooked, and the error of L_0 is in 2.5%-5%. Hence, formula (14) can be simplified as [16-17]:

$$L_0 = \frac{N\left(R_T + \frac{d_2}{2}\right)}{mk_2k_1d_1} \quad (15)$$

When the cable tension is N, and the initial compressed distance of the spring is $L_0 = \frac{N\left(R_T+\frac{d_2}{2}\right)}{mk_2k_1d_1}$, the output shaft II and the planet carrier H face the same moment of resistance. In this case, the two components of the cable reel will have the same active moment, if the motor is powered on.

Let t be the number of seconds for the mobile device to move forward, i.e., the duration of continuous cable pulling by the reel at speed n (Fig. 5). Since the power supply cable follows the single-row multi-layer storage on the reel, the winding radius of the cable will increase at the rate of d_2 mm/turn, as the reel pulls the cable. After t seconds, the winding radius will increase to:

$$R_t = R_T + \frac{d_2}{2} + ntd_2 \quad (16)$$

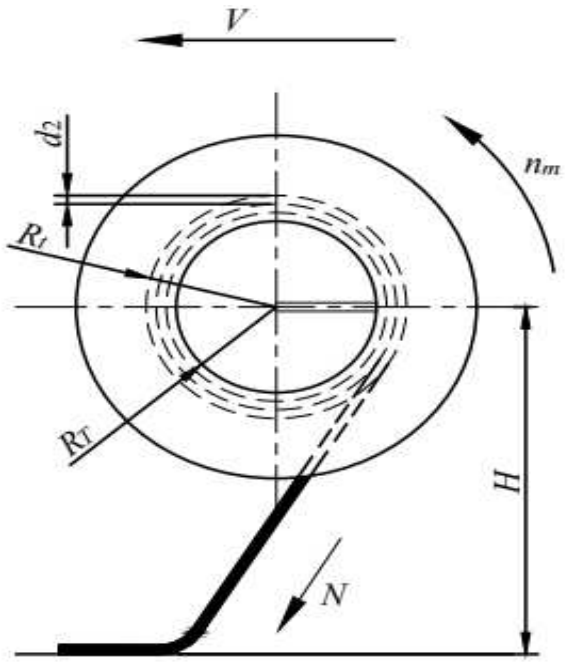

Fig. 5 *Force diagram of device motion*

Suppose the tension is still N when the power supply cable is fully pulled. Then, the moment of resistance of the reel can be expressed as:

$$M'_{T,t} = NR_t = N\left(R_T + \frac{d_2}{2} + ntd_2\right) \tag{17}$$

Without considering the influence of the adjustable big gear over the moment of resistance of the output shaft III, and the frictional loss of the driving chain, the moment of resistance of planet carrier H can be expressed as [9]:

$$M'_{\mathrm{H},t} = M'_{T,t} = NR_t = N\left(R_T + \frac{d_2}{2} + ntd_2\right) \tag{18}$$

Let p be the pitch of the screw-thread pair betweenthe adjustable seat and the adjustable big gear:

$$p = \frac{Nd_2}{mk_2k_1d_1} \tag{19}$$

Because the transmission ratio n_{11-21} from the gear to the adjustable big gear satisfies$\frac{z_{21}}{z_{11}} = 1$, after t seconds, the adjustable big gear moves to the left by a distance of ntp [18]. The total compressed distance L_t (mm)of the spring is $L_t = L_0 + ntp$. According to formula (7), the moment rotating the adjustable big gear is $T_t = k_2k_1L_td_1$. According to formula (8), the friction moment of the friction disk pair, i.e., the moment of resistance of friction disk on the output shaft II can be expressed as:

$$M'_{\mathrm{II}t} = mT_t = mk_2k_1L_td_1 = mk_2k_1d_1(L_0 + ntp) \tag{20}$$

Substituting formulas (15) and (19) into formula (20):

$$M'_{\mathrm{II}t} = N\left(R_T + \frac{d_2}{2} + ntd_2\right) \tag{21}$$

Comparing formula (18) and formula (21), it is clear that $M'_{\mathrm{H},t}$=$M'_{\mathrm{II}t}$. In other words, after the reel has been rotating continuously for t seconds at the speed of n turns/s, if the tension on the fully pulled power supplies the cable remains N, and if the pitch p of the screw-thread pair satisfies formula (19), the planet carrier H and the output shaft II will still have the same moment of resistance. Reversely, after the reel has been pulling the cable continuously for $t$seconds at the speed of n turns/s, if the planet carrier H and the output shaft II still have the same moment of resistance, and if the pitch p of the screw-thread pair satisfies formula (19), the tension on the fully pulled power supply cable will be N. The tension on the cable is N after the reel has been working for t seconds.

The above is the operation principle of our constant tension cable reel.

Formula (19) shows that the pitch p of the screw-thread pair directly hinges on the tension N needed by the cable and the diameter $d_2$of the cable. Hence, the proposed cable reel is specially designed to ensure the constant tension of a specific model of the power supply cable.

4 Operation Mode

First, the initial compressed distance of the spring is determined. When the mobile device is at the start position of the journey, the cable reel belongs to the initial state. Then, one end of the power supply cable is inserted into the reel, passing through the hole of the output shaft III, and connecting with the rotary vane of the collector. Then, the cable will reach the dangling state (Fig. 2).

As shown in Fig. 6, the lever of our cable reel is switched to the left, and the lever will rotate about the shaft and the drive connecting rod. The driver plate will thus move to the right, driving the gear III to slide to the right and disconnect with the adjustable big gear [19-20].

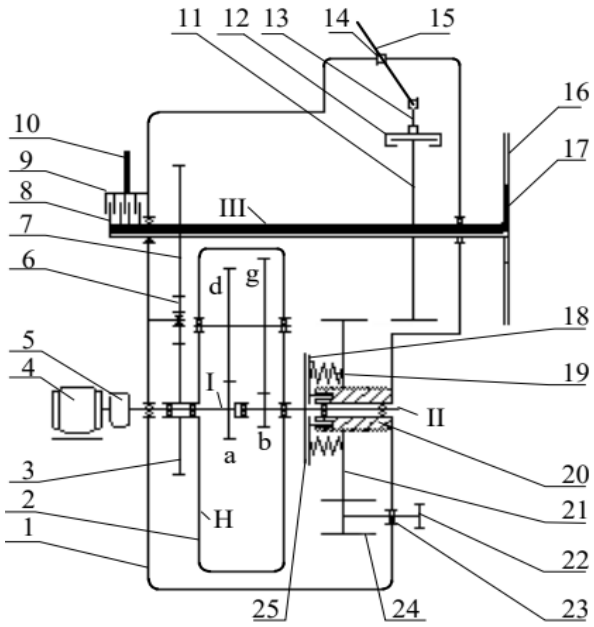

Fig. 6 *Operation mode*

Where:
1…Housing,
2…2K-H (WW) positive differential planetary transmission [5],
3…Gear I,
4…Motor,
5…Worm gear reducer,
6…Transition gear,
7…Gear II,
8…Rotary vane of collector,
9…Static vane of collector,
10…Power line of mobile device,
11…Gear III,
12…Driver plate,
13…Connecting rod,
14…Shaft,
15…Lever,
16…Reel,
17…Power supply cable,
18…Static friction disk,
19…Pressure spring,
20…Adjustable seat,
21…Adjustable big gear,
22…Adjustable hand wheel,
23…Bearing,
24…Adjustable small gear,
25…Rotary friction disk.

Through rotating the adjustable hand-wheel, the adjustable small gear will rotate, causing the adjustable big gear 21 to rotate. Then, the spring will be compressed. Under the spring pressure, the friction disk pair and will produce a moment of resistance to rotate the output shaft II.

For the power supply cable of a specific model, the supposed dangling length L_1 can be calculated when the cable tension is the initial value N (Fig. 4). The reel is rotated manually to pull a bit of the cable, and then releases to rotate freely. Once the dangling length reaches the supposed length L_1, the compressed distance of the spring will be equal to the initial compressed distance L_0. The principle is as follows [21-22]:

When the motor is not energized, the input shaft I will not rotate under the self-locking effect of the worm gear reducer. Then, the rotation of the reel will drive the rotation of the output shaft III, which in turn cause the output shaft II to rotate via the gear II, transition gear 6, gear I, and planet carrier H. Since the transmission ratio from the gear II to the output shaft II $n_{7-\mathrm{II}}$=1, the moment of the output shaft III equals that of the output shaft II, i.e., $M_{\mathrm{III}} = M_{\mathrm{II}}$, meeting the requirement of formula (14). Hence, if the compressed distance of the spring is greater than L_0, then the moment of resistance of the output shaft II will be greater than $M'_{\mathrm{II},0}$. Then, the dangling length of the circle will surely surpass L_1, after the reel 16 is released, and the cable tension must be greater than N. Reversely, if the compressed distance of the spring is smaller than L_0, then the moment of resistance of the output shaft II will be smaller than $M'_{\mathrm{II},0}$. Then, the dangling length of the circle will be less L_1 after the reel is released, and the cable tension must be less than N[23]. The cable tension will eventually reach N after repeated adjustments by the above method. At this point, the compressed distance of the spring is the initial compressed distance L_0.

When the initial compressed distance of the spring is adjusted, the lever is switched to the right, driving the gear III engages with the adjustable big gear. After that, the mobile device can move and the cable reel can start pulling the cable. To ensure the reliability of the cable pulling, the model of the motor, and the worm gear reducer should be selected reasonably at the start position in Fig. 4. Suppose the output shaft II does not rotate, the winding speed of the reel is set to be greater than the moving speed V of the mobile device [24]. As the winding radius of the cable increases, the linear winding speed of the reel will gradually increase, ensuring the reliable pulling of the reel. Therefore, the speed of the motor and the worm gear reducer in the cable reel cannot be adjusted. Under the premise of a static output shaft II, the speed of the output shaft III can be described by $n_{\mathrm{III}0}$(turns/second) at n_{II}=0, according to formula (4) [25].

At the start position in Fig. 4, as the mobile device moves forward at the speed V, when the motor is energized and rotates, the moment of resistance of the planet carrier H equals that of the friction disk on the output shaft II, while the input shaft I allocates equal active moments to the output shaft II and the planet carrier H. Then, both the output shaft II and the planet carrier H will rotate. According to formula (4), the speed n_{III} of the output shaft III must be smaller than $n_{\mathrm{III}0}$. Once the reel speed drops to the speed required to fully pull the cable, the pulled cable will be released, and the moment of resistance of the cable on planet carrier H will decrease [3, 14].

When the gear III drives the adjustable big gear 21 to rotate and move to the left, after a period of time, the moment of resistance of the friction disk pair on output shaft II is always equal to the moment of resistance of drops planet carrier H when the cable is fully pulled [26]. To this end, when the pulled cable is released, the moment of resistance of the planet carrier H will be smaller than that of the output shaft II. Then, the output moment of the output shaft I will decrease, only capable of driving the rotation of the planet carrier H.

When the pulled cable is released, the output shaft II will gradually drop to zero. Under the action of the braking moment of the friction disk pair, the output

shaft III will accelerate to n_{III0}, which boosts the cable pulling. After a period of time, the cable is pulled and its tension reaches N again. Then, the output moment of the planet carrier H becomes equal to that of the friction disk pair on the output shaft II once more. After that, the cable pulling speed of the reel will drop again. The above cable pulling operation will be repeated until the mobile device arrives at the terminal. In this way, the cable always faces a constant tension throughout the pulling process [27].

The above is the flexible pulling process of our constant tension cable reel.

5 Conclusions

A constant tension cable reel is designed based on planetary gear transmission. The structure of the transmission mechanism is designed, and the relationship between the moment and speed is analyzed for each output shaft. The operation mode of the cable reel is explained. The experimental results show that the proposed cable reel can pull the cable flexibly and provide constant tension required by the cable. The proposed device can effectively overcome the problems of existing cable reels, such as chaotic operation and cable damages. However, it should be noted that the pitch of the screw-thread pair is directly related to the required tension of the cable and the cable diameter. This means that if the power supply cable model is different, the parameters of the constant tension cable reel are also different.

Acknowledgement

This work is supported by Key Scientific Research Project Plan for Higher Education, Henan Province, China (Grant No.14B460022) and Key Science and Technology Research Project, Henan Province, China (Grant No.152102210115).

References

[1] LI, H.C., YAN, Z.W. (2018). A flexible retraction cable reel based on planetary gear drive. *Journal Europeen des Systemes Automatises*, Vol. 51, No. 1-3, pp.51-58. DOI:10.3166/jesa.51.51-58

[2] PAL, U., PALIT, P., GOKARN, P., CHATURVEDI, A. (2021). Failure of Cable Reel Flat Spring of Crane: Beyond Fatigue Life Use. *Journal of Failure Analysis and Prevention*, Vol. 21, pp.1257-1263. https://doi.org/10.1007/s11668-021-01160-4

[3] WANG, C. (2020). The effect of planetary gear/star gear on the transmission efficiency of closed differential double helical gear train. *Proceedings of the Institution of Mechanical Engineers, Part C: Journal of Mechanical Engineering Science*, Vol. 234, No. 21, pp.4215-4223. https://doi.org/10.1177/0954406220921205

[4] LI, X., GAO, H.J., WU, Q., WU, S.F., HU, Z., ZHANG, W.H. (2020). Parametric Modeling and Simulation of the Gear Shaping Process of Floating Support Friction Disk. *Proceedings of the 12th International Conference on Computer Modeling and Simulation*, pp. 203-208. https://doi.org/10.1145/3408066.3408074

[5] HU, Q., CHEN, X., XU, Z., MAI, Q., & ZHU, C. (2019). Study on kinematic characteristics of planetary multistage face gears transmission. *Proceedings of the Institution of Mechanical Engineers, Part D: Journal of Automobile Engineering*, Vol. 234, No. 2-3, pp.572-585. DOI: 10.1177/0954407019855908

[6] KUMAR, A., DASGUPTA, K., & KUMAR, N. (2021). Modeling and Analysis of a Novel Priority Valve ControlledCableReeling Drum Drive of Load Haul Dump Vehicle. *IEEE Transactions on Vehicular Technology*, Vol. 70, No. 7, pp. 6636-6646. DOI: 10.1109/TVT.2021.3087541

[7] SAN BENITO PASTOR, D. G., NALIANDA, D., SETHI, V., MIDGLEY, R., ROLT, A., & BLOCK NOVELO, D. A. (2021). Preliminary Design Framework for the Power Gearbox in a Contra-Rotating Open Rotor. *Journal of Engineering for Gas Turbines and Power*, Vol. 143, No. 4, pp.041022. DOI:10.1115/1.4049411

[8] CHEN, X., & YE, W. (2023). Analysis of Factors Affecting Strand Tension in Cable-Twisting Equipment and Method for Equilibrated Control. *Applied Sciences*, Vol. 13, No. 8, pp.4690. https://doi.org/10.3390/app13084690

[9] CHEN, R.Z., LI, X.P., XU, J.C., YANG Z.M., YANG H.X. (2021). Properties Analysis of Disk Spring with Effects of Asymmetric Variable Friction. *International Journal of Applied Mechanics*, Vol. 13, No. 7, pp.2150076. https://doi.org/10.1142/S1758825121500769

[10] ABDERAZEK, H., SAIT, S. M., & YILDIZ, A. R. (2019). Optimal design of planetary gear train for automotive transmissions using advanced meta-heuristics. *International Journal of Vehicle Design*, Vol. 80, No. 2-4, pp.121-136. https://doi.org/10.1504/IJVD.2019.109862

[11] HU, C.F., GENG, G.D., SPANOS, P. D. (2021). Stochastic dynamic load-sharing analysis of the closed differential planetary transmission gear system by the Monte Carlo method. *Mechanism and Machine Theory*, Vol. 165,

pp.104420. https://doi.org/10.1016/j.mechmachtheory.2021.104420

[12] SURÁNYI, M., REINBRECHT, C., & HUEMER, H. (2021). Experimental study of failing differential gears and introduction of a new condition indicator for ultra-low speed applications. *Mechanical Systems and Signal Processing*, Vol. 155, No. 2, pp.107588. DOI:10.1016/j.ymssp.2020.107588

[13] JU, M., XING, X., WANG, L., YUN, F., WANG, X., & LIAO, H. (2021). Numerical Simulations and Experimental Study on the Reeling Process of Submarine Pipeline by R-Lay Method. *Journal of Marine Science and Engineering*, Vol. 9, No. 6, pp.579. DOI:10.3390/JMSE9060579

[14] LIU, S., HU, A., ZHANG, Y., & XIANG, L. (2022). Nonlinear Dynamics Analysis of a Multistage Planetary Gear Transmission System. *International Journal of Bifurcation and Chaos in Applied Sciences and Engineering*, Vol. 32, No. 7, pp.2250096. DOI:10.1142/S0218127422500961

[15] ILIE, F., & CRISTESCU, A. C. (2022). Tribological Behavior of Friction Materials of a Disk-Brake Pad Braking System Affected by Structural Changes-A Review. *Materials*, Vol. 15, No. 14, pp.4745. https://doi.org/10.3390/ma15144745

[16] PROVATIDIS, C. G., KALLIGEROS, C., & SPITAS, V. (2023). Design considerations and simulation of a rolling-contact gearless automotive differential. *Proceedings of the Institution of Mechanical Engineers, Part C: Journal of Mechanical Engineering Science*, Vol. 237, No. 20, pp.09544062231154080. https://doi.org/10.1177/09544062231154080

[17] PHADATARE, H. P., & PRATIHER, B. (2020). Dynamic stability and bifurcation phenomena of an axially loaded flexible shaft-disk system supported by flexible bearing. *Proceedings of the Institution of Mechanical Engineers, Part C: Journal of Mechanical Engineering Science*, Vol. 234, No. 15, pp.2951-2967. DOI:10.1177/0954406220911957

[18] LIU, Y., LI, J., WANG, T., DING, Y., & WANG, G. (2022). Study on the friction resistance calculation method of a flexible shaft of wire rope based on genetic algorithm. *Mechanics of Advanced Materials and Structures*, Vol. 29, No. 19, pp.2836-2844. DOI:10.1080/15376494.2021.1879329

[19] GE, H., SHEN, Y., ZHU, Y., XIONG, Y., YUAN, B., & FANG, Z. (2021). Simulation and experimental test of load-sharing behavior of planetary gear train with flexible ring gear. *Journal of Mechanical Science and Technology*, Vol. 35, No. 11, pp.4875-4888. DOI:10.1007/s12206-021-1006-1.

[20] YAO, J., DENG, X., MA, C., & XU, T. (2021). Investigation of Dynamic Load in Superdeep Mine Hoisting Systems Induced by Drum Winding. *Shock and vibration*, Vol. 2021, pp.4756813. https://doi.org/10.1155/2021/4756813

[21] GRIFFIOEN, W., & PLUMETTAZ, D. (2021). Cable Pulling Force in Pipes with 3D Bends for Different Installation Methods. *Journal of Pipeline Systems Engineering and Practice*, Vol. 12, No. 4, pp.04021060. DOI:10.1061/(asce)ps.1949-1204.0000607

[22] QUAN, W.C., CHANG, Q.Q. (2020). Variable-Length Cable Dynamics of Payout and Reel-in with a Vertically Tethered Underwater Drill Rig. *IEEE Access*, Vol. 8, pp.66625-66637. DOI: 10.1109/ACCESS.2020.2984752

[23] SÍŤAŘ, V., VYSLOUŽIL, T., RAKOVÁ, L., & HRUŠKA, T. (2021). The power load model for electric vehicle charging modelling and its utilisation for voltage level studies and cables ampacity in distribution grid. *Manufacturing Technology*, Vol. 21, No. 1, pp. 132-140. DOI: 10.21062/mft.2021.015

[24] MAMOŃ, F., JASKEVIČ, M., MAREŠ, J., NOVOTNÝ, J. (2023). Fire Resistance Test of Geopolymer Coatings on Non-Metallic Underlying Substrates. *Manufacturing Technology*, Vol. 23, No. 2, pp. 225-232. Doi: 10.21062/mft.2023.026.

[25] TORRES CHARRY, G., & GÓMEZ MENDOZA, J. B. (2021). An Experimental Test Bench for Cable-Driven Transmission. *Machines*, Vol. 9, No. 5, pp. 83. DOI:10.3390/machines9050083

[26] ZHANG, L., ZHENG, T., LI, T., WANG, J., WANG, C., JIANG, Y., LI, C., YUAN, F., YAO, Z. (2023). Precision Forming Process Analysis and Forming Process Simulation of Integrated Structural Gear for New Energy Vehicles. *Manufacturing Technology*, Vol. 23, No. 6, pp. 958-966. Doi: 10.21062/mft.2023.102.

[27] MA, T.L., WEI, Z.H., WANG, X.S., CHEN, H.B. (2019). Simulation of the reel-in operation of towed target system with constant-length method. *AIAA Scitech 2019 Forum*. https://doi.org/10.2514/6.2019-0437